

Study of the Electronic Properties of Matched Na-containing and Na-free CIGS Samples Using Junction Capacitance Methods

Peter T. Erslev¹, Adam F. Halverson¹, J. David Cohen¹, and William N. Shafarman²

¹ Department of Physics, University of Oregon, Eugene, OR 97403 U.S.A.

² Institute of Energy Conversion, University of Delaware, Newark, DE 19716 U.S.A.

ABSTRACT

Junction capacitance methods were used to examine a matched pair of Cu(In_xGa_{1-x})Se₂ (CIGS) thin film solar cells, one with Na incorporated into the absorber and the other with a diffusion barrier to inhibit the Na incorporation from the soda-lime glass. Typical cells showed a 50% increase in efficiency with the addition of Na to the devices. Forward biased admittance spectroscopy revealed a large defect density located near the CdS/CIGS heterojunction in the Na-less samples not present in the Na samples. This defect may be responsible for the loss in V_{oc} which contributes to the loss in efficiency when Na is not added to the devices. Drive Level Capacitance profiles revealed free carrier densities of $3 \times 10^{14} \text{ cm}^{-3}$ and $1.1 \times 10^{14} \text{ cm}^{-3}$ for the Na and Na-less samples, respectively. Transient photocapacitance spectra also showed interesting differences between the samples, but nothing significant enough to account for the magnitude of loss in efficiency.

INTRODUCTION

Thin film photovoltaic devices have the potential to provide an inexpensive renewable source of electrical power. Polycrystalline Cu(In_xGa_{1-x})Se₂ (CIGS) materials is one of the most promising, with the highest efficiency ($\eta = 19.4 \%$) reported for a thin film solar cell [1]. The addition of Na to the CIGS absorber layer is a commonly followed procedure, boosting the efficiency by up to 50% primarily through a sizeable increase in the open-circuit voltage (V_{oc}) and the fill factor (FF). Although the positive role of Na is well known, there is an ongoing debate as to the exact mechanism of the beneficial effect of Na.

Most of the debate centers around where in the cell the Na has an effect on the performance of the device. Possible sites are grain boundaries, in the bulk of the grains, or the CdS/CIGS heterojunction. Recently published experimental results have been contradictory, with one group finding no evidence of Na at the grain boundaries[2] and another group concluding that the Na is only found in significant amounts at the grain boundaries[3]. Another hypothesis is that the Na acts only during the growth of the sample to organize and passivate point defects[4]; however, this is disputed by similar benefits obtained through diffusion of Na into the sample in a post-deposition treatment[5].

In this paper we present results from junction capacitance measurements performed on a pair of co-deposited CIGS sample devices, one with Na and the other with a diffusion barrier to inhibit the movement of Na from the soda-lime glass substrate into the absorber layer. These have been investigated with junction capacitance methods including admittance spectroscopy, drive-level capacitance profiling (DLCP) and transient photocapacitance (TPC) spectroscopy. Somewhat to our surprise the differences that our measurements have revealed on the CIGS absorber properties were not sufficient to account for the nearly 50% difference in efficiency of the two devices. Instead, the differences in performance appear to be directly linked to differences near the barrier interface of the two kinds of devices.

SAMPLES

The pair of matched baseline (34017.12) and reduced Na (34017.32) samples were provided by the Institute of Energy Conversion. The samples were co-deposited at 550°C in a single deposition with a thickness of 2.0 μm . The baseline film was deposited on a Mo-coated soda lime glass substrate and the reduced Na film was deposited on a substrate provided by Shell Solar which has a SiO_2 diffusion barrier below the Mo. Both devices were completed with standard CdS, ZnO and ITO depositions and a Ni/Al grid. Table I provides the device performance parameters of the cells analyzed and discussed below. These parameters were typical for all of the cells on the samples. The differences between these samples exhibit the commonly known effects of Na on CIGS solar cells: An increased V_{oc} , fill factor, and efficiency (by nearly 50%), with virtually no effect on short circuit current.

Table I: Device performance parameters of the matched CIGS devices with and without Na.

Cell	V_{oc} (V)	J_{sc} (mA)	FF (%)	Eff (%)
34017.12 – 1 (Na)	0.624	32.9	74.0	15.2
34017.32 – 4 (Na-less)	0.494	33.6	64.3	10.7

CHARACTERIZATION METHODS

Admittance spectroscopy examines the complex electrical response of the device to an ac-perturbing voltage over a range of frequencies and temperatures. The frequency and temperature of the measurement define an emission energy $E_c = k_B T \ln(v/2\pi f)$ where k_B is Boltzmann's constant, T is the temperature of the measurement, v is the thermal emission prefactor, and f is the measurement frequency.

Drive-level capacitance profiling (DLCP) is used to determine deep defect density by examining the non-linear capacitive response of the junction capacitance ($C = C_0 + C_1 \delta V + C_2 (\delta V)^2 + \dots$) as a function of the amplitude, δV , of the applied oscillating voltage. The drive level density, N_{DL} , is obtained from the coefficients C_0 and C_1 and it is directly related to the free carrier density plus an integral over the density of deep defect states to an energy E_c above E_V , and near the spatial position $\langle x \rangle = \varepsilon A / C_0$ from the barrier junction[6]. Spatial profiles are obtained by varying the dc reverse bias.

The transient photocapacitance (TPC) method was used to obtain sub-band-gap optical absorption-like spectra. A sample is held at reverse bias and is periodically pulsed to zero or slightly forward bias to “reset” the occupation of defects within the sample; i.e., to let majority carriers into the previously empty traps in the depletion region. After the pulse is removed, a capacitance transient is observed as the carriers are thermally emitted from the occupied traps. The TPC signal is obtained by comparing the transient while the sample is illuminated with sub-bandgap monochromatic light to the transient while the sample is in the dark. By varying the wavelength of the monochromatic light we obtain a TPC spectrum, and it is closely related to an integral over the density of states in the band-gap, as has described in detail elsewhere[7].

One important feature exhibited in such TPC spectra is the exponential distribution of bandtail states near the band edges. The slope of these bandtail states is characterized by an Urbach energy which increases with increasing structural and compositional disorder within the material. The TPC spectra also disclose the presence of one or more bands of defect states deeper within the gap, which are typically well fit by gaussian distributions.

EXPERIMENTAL RESULTS

Drive-level capacitance profiles are displayed for the CIGS samples with and without Na in Fig. 1. These profiles were obtained at 10 kHz for a variety of temperature with applied biases ranging from at least 1.0 V reverse to 0.3 V forward. The profiles in Figure 1 show similar overall shapes but more spatial variation in the sample with Na. The sample with Na shows a defect activating between 130 K and 190 K that is absent in the Na-less sample. Without any prior knowledge of cell performance, one would predict that the more spatially uniform sample without evidence for deeper states, the Na-less sample, to be more efficient. Since exactly the opposite is true, this indicates that something not visible in the DLC profiles is having a dramatic harmful effect on the performance of the low Na cell.

These profiles indicate free carrier densities of $3 \times 10^{14} \text{ cm}^{-3}$ for the Na sample and $1.2 \times 10^{14} \text{ cm}^{-3}$ for the Na-less sample. From the higher temperature profiles we infer a deep acceptor density of $\sim 1 \times 10^{15} \text{ cm}^{-3}$. The Na-less sample does not show this type of defect, instead it increasing only slightly with temperature to a maximum value of $\sim 3 \times 10^{14} \text{ cm}^{-3}$. The abrupt increase in the DLC profiles near the junction ($\langle x \rangle = 0$) may reflect a significant defect density near the junction, however we are not certain whether the DLCP can provide an accurate measurement of the defect density is accurate in this region. We thus choose to use the more spatially uniform region of the profiles to estimate the free carrier and defect densities.

In Fig. 2 we compare the TPC spectra for the Na and Na-less samples. The spectra have been aligned above the 1.2 eV gap energy to enable a better comparison. Much like the DLC profiles, the spectra are surprisingly similar. The thin solid lines indicate fits in which we have assumed a gaussian defect band and an exponential band tail. The sample containing Na exhibits an Urbach energy of 17 meV plus a gaussian defect band centered at 0.75 eV above E_V with a variance of 60 meV. The Urbach energy for the low Na sample is larger, 23 meV, and the gaussian defect band appears centered at 0.70 eV with a much smaller variance, about 25 meV. The narrower bandtail for the sample with Na suggests a higher degree of crystalline order within the CIGS absorber[8].

Admittance spectra were obtained for each of these samples for frequencies between 100 Hz and 100 kHz and temperatures between 80 K and 280 K. With 0 V applied bias, there is a very distinct activated step in the sample with Na and no clear feature in the Na-less

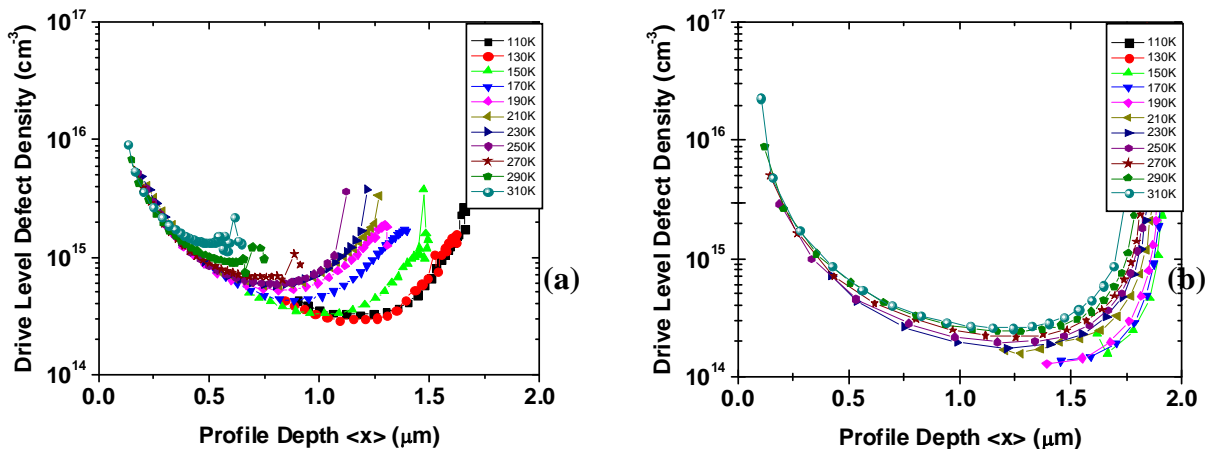


FIG. 1. DLC Profiles for a) Na and b) Na-less samples. The profiles have very similar shapes, and the Na sample appears to be less spatially uniform, which might suggest a poorer performing solar cell. However, this is not the case, and the Na cell is 50% more efficient than the Na-less.

sample, as shown in Figure 3 (a) and (b). The step in the Na sample has an activation energy of 270 meV as determined by an Arrhenius plot, consistent with many previous admittance measurements of CIGS materials. It is worth pointing out that this many researchers have associated a larger step in admittance with poorer device performance. However, in this case, exactly the opposite is true.

Admittance spectra were then obtained over the same frequency ranges, but with an applied bias. Under reverse bias of 0.5 V, there were no changes in the spectra. The Na-less sample spectra looked the same, and the magnitude of the step in the Na sample spectra changed in the manner expected for a bulk defect. The surprise came when the admittance spectra were obtained under forward bias. The Na-less sample showed a clear activated step, and the Na sample showed only a hint of an additional step, as shown in Fig. 3(c) and (d). For the admittance data of Fig. 4, in which we varied the forward bias while keeping the temperature constant, one sees the further development of this effect. The Na sample

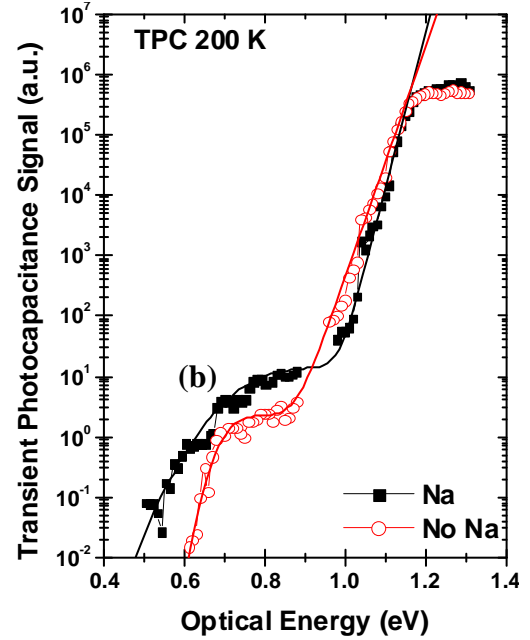


FIG. 2. TPC Spectra of the two samples. The Na-less sample spectrum exhibits a broader bandtail, indicating a higher level of disorder for that sample.

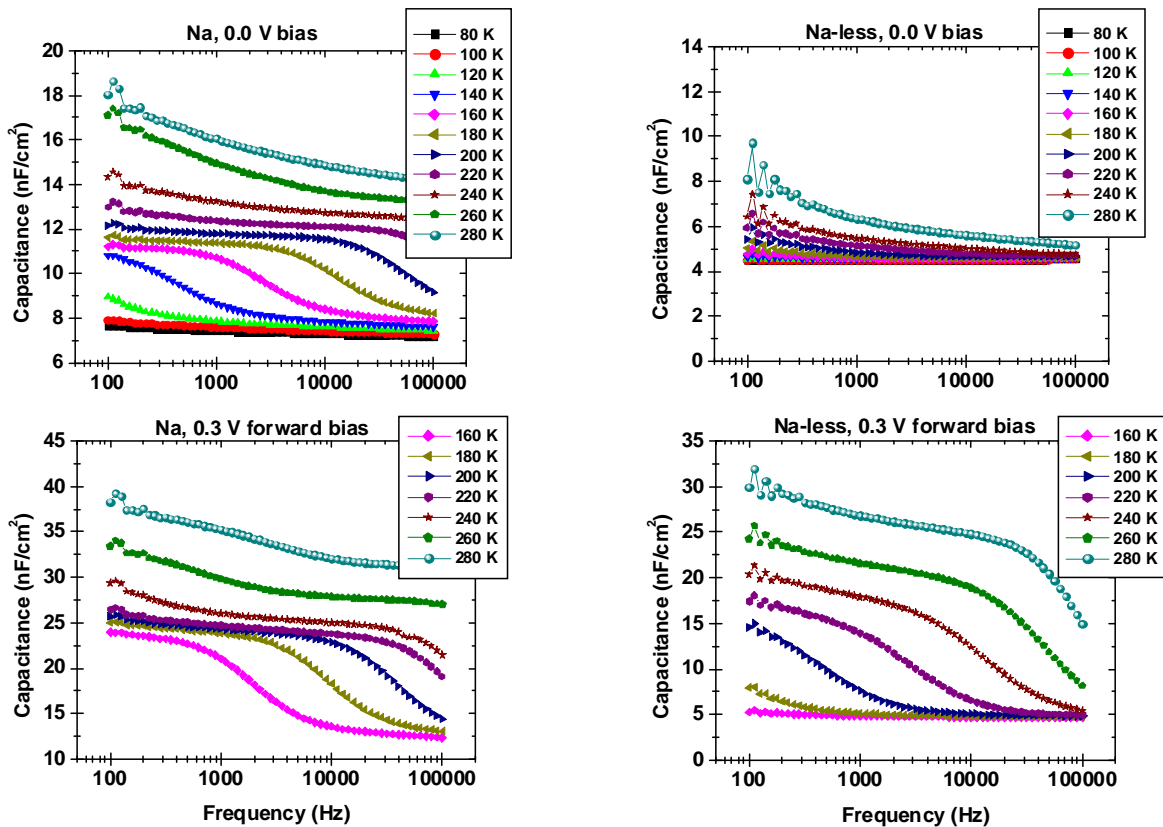


FIG. 3. Admittance spectra for (a) & (c) the Na containing sample, and (b) & (d) the Na-less sample. The Na-less sample shows a step which only is visible under an applied forward bias.

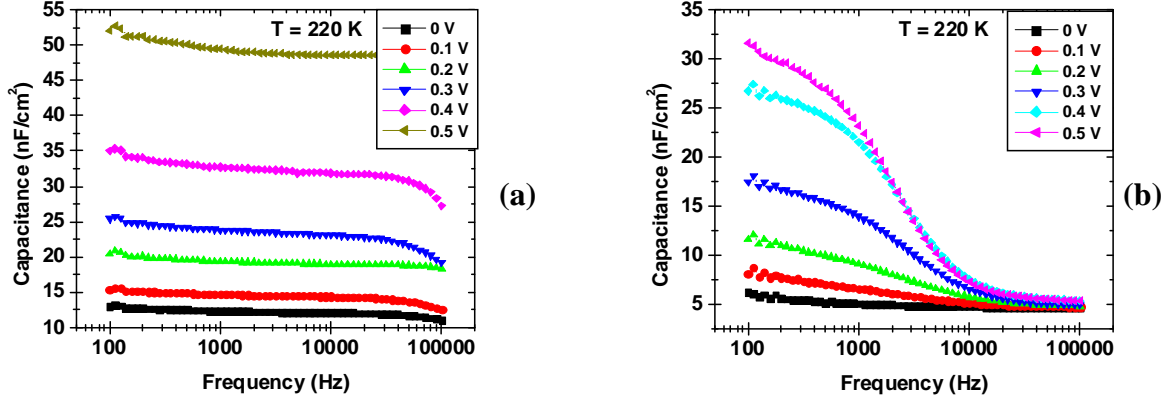


FIG. 4. Admittance vs applied voltage for (a) Na sample, 280 K and (b) Na-less sample, 220 K. The appearance of the capacitive step under forward bias and the limit in its magnitude for the Na-less sample are both characteristic responses of an significant interface state.

showed perhaps a hint of a step at 280 K, however this step was relatively very small. In contrast, the Na-less sample showed a very clear step between 180 K and 300 K which had an activation energy of 380 meV.

DISCUSSION

The behavior displayed in Figure 4 clearly indicate the presence of large density of states near the interface for the Na-less sample compared to the sample with Na. First, the capacitance of the Na sample is able to increase without any apparent bound with applied forward bias, whereas the Na-less sample looks like it will reach a limit near 35 nF/cm^2 . This limit suggests that something is preventing the depletion region from collapsing any further under forward bias, such as a defect at the interface that becomes more and more charged with increasing forward bias. The fact that the step is only visible over a limited bias range also indicates that this defect is located in the interface. This feature is by far the most profound difference between the Na and Na-less samples, so it seems reasonable that it is this is the most likely candidate to explain the difference in performance of the two samples.

Indeed, a sufficient large defect density in close proximity to the CdS/CIGS interface could easily affect the band bending and result in the 130 mV observed difference in V_{oc} . If we assign this open circuit voltage loss exclusively to this defect, then by integrating Poisson's equation, we can estimate the amount of extra charge that is accumulating near the interface.

Namely,

$$\Delta V = \frac{1}{\epsilon_0} \int_0^{\infty} x \rho(x) dx \approx \frac{q N_{int} d}{\epsilon}, \quad (1)$$

where $q N_{int}$ is the total sheet charge density present near the open circuit voltage condition, and d is the width of its spatial distribution from the barrier interface. For example, if we assume that d is 50 nm, then a 0.13 difference in the device voltage requires a change of sheet charge density $1.6 \times 10^{11} \text{ cm}^{-2}$.

We can also try to reconcile this estimate with the results of our admittance and DLCP measurements discussed above. Figure 5 shows numerical calculations in which we place a deep defect of areal density near 10^{12} cm^{-2} within roughly $0.2 \text{ } \mu\text{m}$ of the barrier interface, broadly distributed in energy. The change in its occupation over the range of the open circuit voltage is then quite close to the above estimate. It is then possible to closely reproduce both the drive-

level profiles and the admittance curves under forward bias exhibited by the Na-less sample.

CONCLUSIONS

We have used junction capacitance methods to study the effect of Na on CIGS thin film solar cells. Our DLCP measurements revealed an increased free carrier density with the addition of Na and an activated bulk defect in CIGS absorber. However, neither can account for the 50% increase in efficiency with the addition of Na. The sub-band-gap TPC spectra showed a broader defect band and a steeper Urbach energy with the addition of Na. The narrower bandtail indicates that Na leads to an increase in the carrier mobilities, but this

again is not expected to lead to differences in performance consistent with the observations. Ultimately, the forward bias admittance measurements revealed the largest differences between the two samples. These data indicate the existence of a large defect density at the CdS/CIGS heterojunction. The conclusion that this defect is not present in the bulk absorber region is corroborated by the lack of any defect response in the corresponding DLC profiles. Finally, we argue that such a defect could readily explain the loss in V_{OC} in the sample with reduced Na, and would be consistent with the observed admittance and DLCP behavior for this sample. Thus we conclude that it is the passivation of this interfacial defect that appears to be the primary contribution of Na to the performance of the CIGS solar cells fabricated at IEC.

ACKNOWLEDGEMENTS

This research was supported by the NREL Thin Film Partnership Program under Subcontract ZXL-5-44205-11 at Oregon and XAT-4-33624-01 at Delaware. We also wish to thank Matt Young and Sally Asher at NREL for SIMS measurements.

REFERENCES

1. K. Ramanathan, M.A. Contreras, C.L. Perkins, S. Asher, F.S. Hasoon, J. Keane, D. Young, M. Romero, W. Metzger, R. Noufi, J. Ward and A. Duda, *Prog. Photovolt.* **11**, 225 (2003).
2. C. Lei, C.M. Li, A. Rockett and I.M. Robertson, *J. Appl. Phys.* **101**, 024909 (2007).
3. V. Lyahovitskaya, Y. Feldman, K. Gartsman, H. Cohen, C. Cytermann, and David Cahen, *J. Appl. Phys.*, **91**, 4205 (2002).
4. A. Rockett, *Thin Solid Films* **480-1**, 2 (2005).
5. D. Rudmann, D. Bremaud, H. Zogg and A. N. Tiwari, *J. Appl. Phys.* **97**, 084903 (2005).
6. J.T. Heath, J.D. Cohen, and W.N. Shafarman, *J. Appl. Phys.* **95**, 1000 (2004)
7. J.D. Cohen, J.T. Heath, and W.N. Shafarman, in *Wide Gap Chalcopyrites*, ed. by U. Rau and S. Siebentritt, (Springer, Berlin, 2005), pp. 69-90
8. S.M. Wasim, C. Rincon, G. Marin, P. Bocaranda, E. Hernandez, I. Bonalde and E. Medina, *Phys. Rev. B.*, **64**, 195101 (2001).

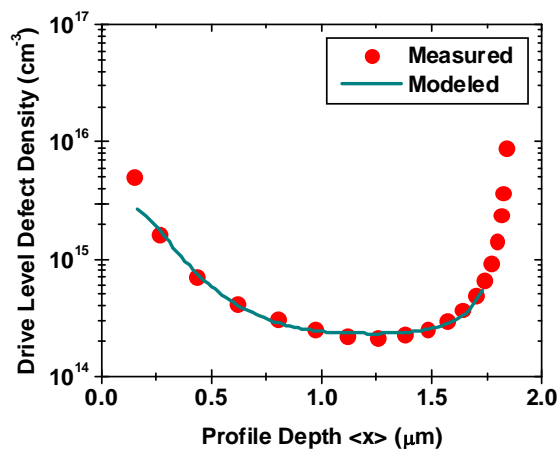


FIG. 5. Comparison of experimental Na-less DLC profile (solid circles) with a calculation (line) based upon an assumed distribution of defects near the barrier interface.